RADIATIVE-CONVECTIVE PROCESSES IN REGULATING TROPICAL OCEAN-ATMOSPHERE

Chung-Hsiung Sui*, Ming-Dah Chou, Ka-Ming Lau
NASA/Goddard Space Flight Center, Greenbelt, Maryland

1. INTRODUCTION

Relationship between sea surface temperature (SST) and cloud/water vapor reveals important information about radiative-climate feedbacks. Many previous studies have shown that cloud amount and SST are positively correlated for SST between 28-29.5°C, For SST>29.5°C, cloud amount actually decreases with increasing SST (e.g. Gadgil et al. 1984, Graham and Barnet 1987, Waliser 1996, Lau et al. 1997). Waliser (1996) suggested that the breakdown of SST-cloud correlation at 29.5°C may be related to the formation of localized hot spots with very high SST due to increased solar radiation in regions of strong subsidence forced by convection elsewhere. In this study, the breakdown is related to the radiative cooling in the subsidence regime over the cold pool surrounding the warm pool. We show model and observational evidence that radiative cooling over the cold pool limits the strength of SST-induced tropical circulation. As a result, occurrence of convection is also limited when SST contrast between the warm pool and cold pool is large. The above regulation mechanism is also applied to discuss a negative relationship between cloudy area and SST (Chou 2000). This is used by Lindzen et al. (2000) as supporting evidence for a SST-cloud/water vapor feedback mechanism.

2. MODEL RESULTS

SST-convection relationship in the tropical deep convective regime and the surrounding subsidence regime is investigated in a cumulus ensemble model (CEM). The model is constrained by an imposed warm-pool and cold-pool SST contrast (dSST). The domain-mean vertical motion is also constrained to provide a heat sink and moisture source in the model to emulate the observed tropical climate condition. In a series of experiments, the warm pool SST is specified at different values while the cold pool SST is specified at 26°C. A circulation with mean ascending (descending) motion over the warm (cold) pool is developed in all experiments. The strength of the circulation increases with increasing dSST until dSST reaches 3.5 °C (Exp. R to R1), and remains unchanged as dSST exceeds 3.5°C (Exp. R1 to R2). The change in circulation and corresponding changes in temperature and humidy is summarized in Fig. 1. This can be explained by the change in heat budget in the subsidence regime where radiative cooling changes little. For dSST<3.5°C, an enhanced subsidence warming is balanced by a reduced condensation heating. For dSST>3.5°C, the subsidence regime becomes too stable for condensation heating to occur so that a further enhanced subsidence warming can no longer be sustained.

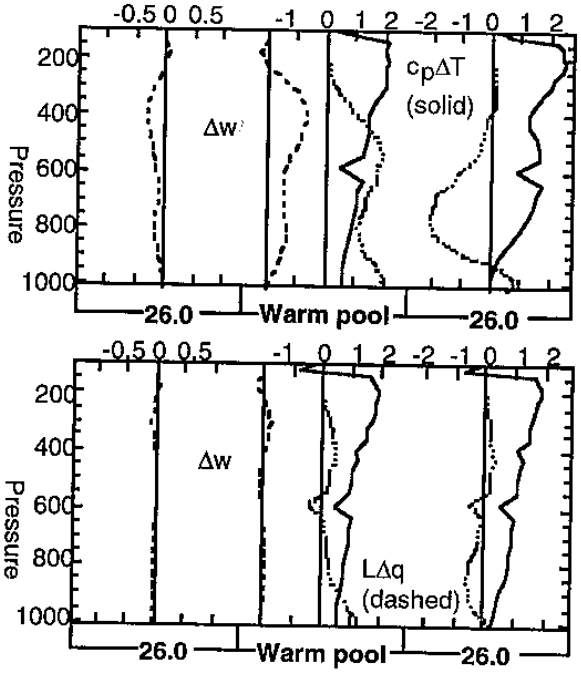

Fig. 1 Difference of ensemble mean temperature, humidity, and vertical velocity between R1-R (upper) and R2-R1 (lower) over the warm pool and cold pool. Units of C_pT and Lq are Jg^{-1}, w is $cm\ s^{-1}$

The regulation of SST-induced circulation by radiative cooling affects the change of clouds as shown in the Table below. Clouds in the model are classified into three types: convective raining, stratiform raining, and stratiform non-raining, and their corresponding spatial coverage are denoted by A_{CR}, A_{SR}, and A_{SN}, respectively. The table shows that the change of active clouds (A_{CR+SR}) is closely

* Corresponding author address: C.-H. Sui, Code 913, Goddard Space flight Center, Greenbelt, MD 20771; E-mail: sui@climate.gsfc.nasa.gov

related to the change of local circulation. For dSST<3.5°C (R1-R1), the enhanced circulation leads to an increase of A_{CR+SR} by 1.7% over the warm pool and a decrease of A_{CR+SR} by 2.6% over the cold pool. For dSST>3.5°C (R2-R1), circulation remains almost the same and the change of A_{CR+SR} is much weaker (-0.4% over the warm pool and 0.1% over the cold pool). Another important feature is the change of passive clouds (A_{SN}). Since A_{SN} consists of high clouds (above 500 hPa) originated from convective clouds, the change of A_{SN} is related to the change of active clouds in addition to the local circulation change. For dSST<3.5°C, A_{SN} over the cold pool increases by 4.5% despite the stronger downward motion, due to the increased A_{CR+SR} over the warm pool. The increase active clouds further lead to a decreased A_{SN} over the warm pool through enhanced mesoscale downdrafts. For dSST>3.5°C, the change of A_{SN} over the cold pool is significantly smaller (0.6%) due to the small change of circulation. In another experiment (W), the warm pool and cold pool temperature are specified 1°C warmer than those of R so the dSST remains at 2.5°C. The 4.4% increase of A_{SN} over the cold pool between W and R is apparently related to the increase of A_{CR+SR} over the warm pool. Finally, we note that total cloud amount (A_T) increases with increasing SST when dSST<3.5°C assuming the domain averaged circulation remains the same. This relation breaks down when dSST>3.5°C.

Table Fractional area of clouds (%)

	Warm Pool		Cold pool		Total
	A_{CR+SR}	A_{SN}	A_{CR+SR}	A_{SN}	A_T
R1-R	1.7	-0.6	-2.6	4.5	3.0
R2-R1	-0.4	-0.3	0.1	0.6	-0.1
W-R	0.4	0.8	-1.9	4.4	3.8

3. OBSERVATIONS

To seek supporting evidence for the model results, we analyze monthly-mean values of high cloud amount (A_{HC}), total precipitable water (W), and vertical p-velocity (ω) as a function of SST. High cloud is derived from ISCCP D2 for the period July 1983 - August 1994 with a spatial resolution of 2.5°x2.5° longitude-latitude. A_{HC} is defined to be the cloud at levels higher than 440 hPa (Rossow and Schiffer 1991). Total precipitable water is derived over the oceans from measurements of the Special Sensor Microwave/Imager (SSM/I) on the DMSP F-8 satellite (Greenwald et al. 1993). The products are limited to water surfaces because ocean surface emissivities at microwave frequencies are low enough to provide a sufficiently cold background for a reliable retrieval of water vapor and liquid water. The data are made of monthly mean quantities on 1°x1° longitude-latitude grid from July 1987 to December 1998. Vertical p-velocity is obtained from NCEP/NCAR data assimilation. The NCEP/NCAR has a horizontal resolution of 2.5°x2.5° longitude-latitude and available for 1949-1999 at present (Kalnay et al. 1996). The optimum interpolation SST is the merged ship and satellite observations by Reynolds and Smith (1994). The SST is available on a T62 Gaussian grid (~1.87°x1.87° longitude-latitude). To be consistent with ISCCP D2 high cloud and NCEP/NCAR vertical velocity, the horizontal resolution of SSM/I precipitable water and SST is degraded to 2.5°x2.5° longitude-latitude by linear interpolation.

The tropical Pacific within 20°S-20°N, 130°E-110°W is chosen as our analysis domain. Within it, warm pool and cold pool is separated by an isotherm so determined that the area of warm pool is 25% of the analysis domain. The area averaged SST over the warm pool and cold pool are plotted against their corresponding difference (dSST) in Fig. 2. The strong negative relation

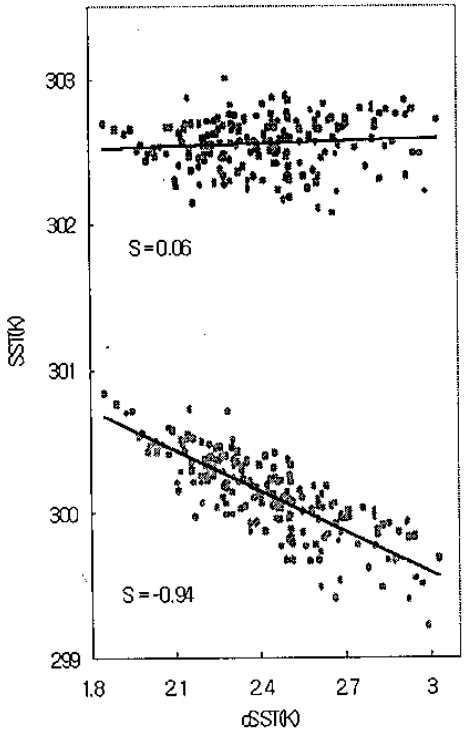

Fig. 2 The area averaged SST over the warm pool and cold pool as a function of dSST.

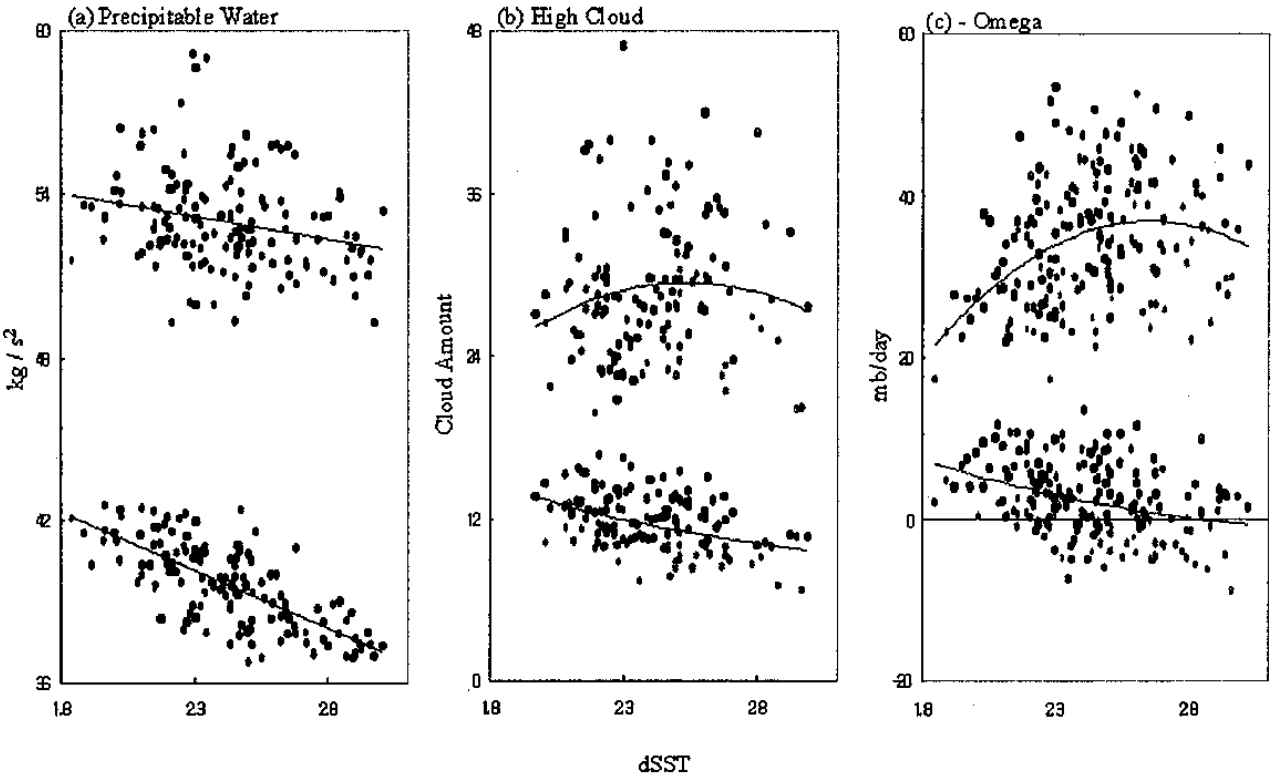

Fig. 3 Scatter plot of W (a), A_{HC} (a), and $-\omega$(500 hPa) over the warm pool (upper) and cold pool (lower) as a function of dSST. Red, green, and blue circles correspond to the three categories of ω

between cold pool SST and dSST is contributed by the ENSO evolution (figure not shown). The weak positive relationship between warm pool SST and dSST indicates the significant contribution by seasonal cycle in addition to the ENSO evolution.

Mean A_{HC} over the warm pool and cold pool as a function of dSST is shown in Fig. 3b. A_{HC} over the warm (cold) pool appears to be positively (negatively) correlated with dSST for dSST<2.6°C. This correlation is related to the increased ascending (descending) motion over the warm (cold) pool associated with enhanced dSST as shown by the $-\omega$ at 500 hPa level in Fig. 3c. The correlation breaks down for dSST>2.6°C, consistent with the modeling results discussed above. Note that the different threshold of dSST between the model results and observations is primarily due to the different area ratio between warm pool and cold pool. Figure 3 also shows a negative W-dSST relationship over the cold pool, as expected in the subsidence regime. However, W and dSST over the warm pool appears to be negatively correlated. In comparison of the above analysis with model results, we note that, unlike the model experiments, the mean vertical motion in the domain of analysis varies and is expected to influence the SST-cloud/water vapor relationship. To further clarify the results, A_{HC}, W, and ω in Fig. 3 are shown in three categories of ω at 500 hPa: $(\omega-\omega_m)<-2$ mbday^{-1} (red), $|\omega-\omega_m|<2$ mbday^{-1} (black), and $(\omega-\omega_m)>2$ mbday^{-1} (blue), where ω_m is the time mean ω. The circulation-stratified A_{HC} and W as a function of dSST shows several important features. First, A_{HC} and W is generally highest in category 1 and lowest in category 3. Second, A_{HC}-dSST relationship discussed above is more evident in each category. Third, A_{HC} and W are positively correlated, and W-dSST relationship is similar to the A_{HC}-dSST relationship except for weak dSST(<2.3°C). The overall observational evidence is consistent with model results.

To link the above analysis with the SST-cloud relationship discussed above, we show the scatter plot of collocated A_{HC} and SST grid values for all dSST, dSST>2.7°C and dSST<2.2°C (Fig. 4). The change of relationship between SST and mean A_{HC} at 29.5°C is evident for the cases dSST>2.7°C, but not so for the cases dSST<2.2°C, suggesting a regulation by radiative cooling in the large subsidence region over the cold pool.

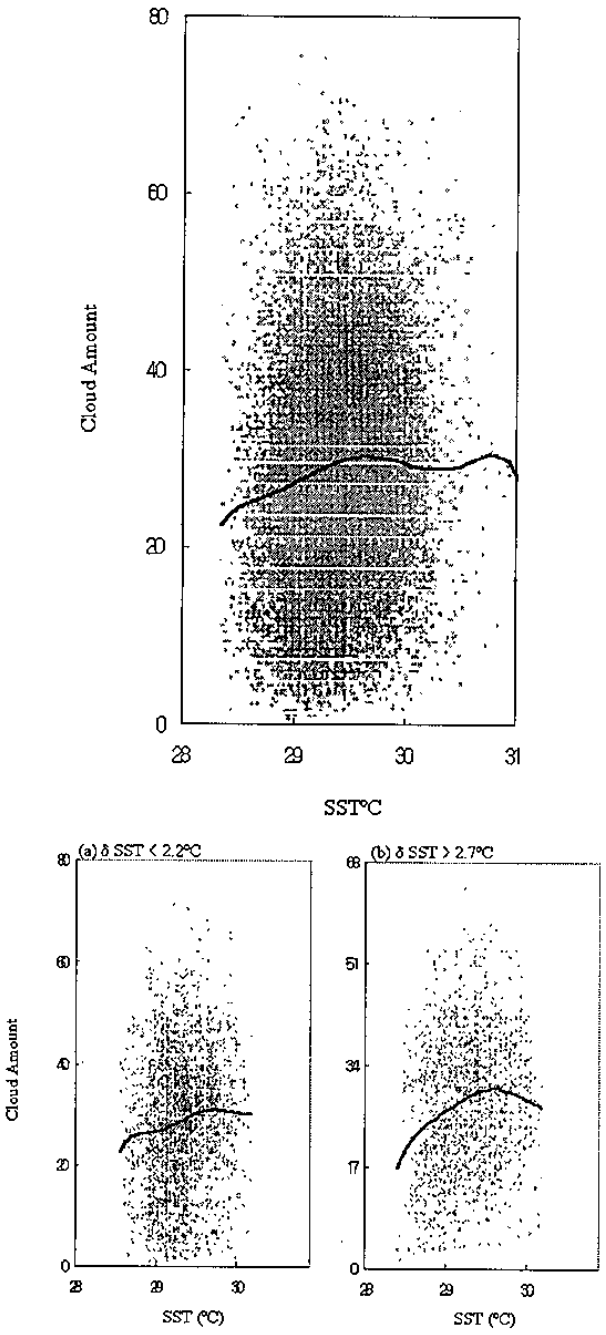

Fig. 4 Scatter plot of collocated SST and A_{HC} in the tropical Pacific (20°S-20°N, 130°E-110°W) for (a) all dSST, (b) dSST> 2.7°C, and (c) dSST< 2.2°C. Superimposed are the mean A_{HC} values within every 0.2°C SST bin

4. CONCLUSION AND DISCUSSION

Our CEM experiments and observational analysis reveal a regulation mechanism of tropical convection by radiative cooling in the broad subsidence regime surrounding the warm pool. Warmer SST in the warm pool (and/or colder SST in cold pool) normally leads to increased occurrence of convection over the warm pool due to SST-induced circulation. This tendency breaks down when the SST gradient becomes large and sinking motion over the cold pool cannot increase anymore as constrained by radiative cooling. In such situation, the area ratio of cloudy area to clear area over the warm pool reduces to maintain mass and energy balance.

The above mechanism is relevant to a negative relationship between cloudy area as measured by the Japanese GMS-5 geostationary satellite, and the cloud-weighted SST by Chou (2000). They showed a 15% reduction in cloudy area for a 1°C increase of the SST. Our model results show 6-11% increase per 1°C increase of SST in case dSST is not too strong. For strong dSST, however, a slightly negative (-0.3 %) change per 1°C increase of SST is found. To examine whether this is evident in observations, we examined the scatter diagram of mean A_{HC} over the domain (20°S-20°N, 130°E-110°W) as a function of cloud-weighted SST and found a similar negative cloud-SST relationship as found by Chou (2000). However, the A_{HC}-SST plot in different categories of dSST shows that the negative relationship becomes less evident in weak dSST category (figure not shown). The cause of the cloud change with SST is attributed by Lindzen et al (2000) to microphysics, i.e. coalescence proceeds more rapidly with increasing air temperature (linked to SST) and results in a reduced cirrus outflow. Our results indicate that the cause of the cloud change involves cold pool radiative cooling in addition to microphysics. The difference rate of change between model and observation may be related to model deficiencies (2D not 3D, limited domain size) and idealized constraints in the experiments. On the other hand, intraseasonal variability and the SST induced convergence may contribute to the observed correlation.

The change in area ratio between cloudy and clear areas in response to SST changes may have profound impact on radiation-climate feedback as suggested by Lindzen et al. (2000). In our CEM experiments, the change of water vapor and cloud greenhouse effect (G_{clear}, C_{LW}) per degree increase of dSST is about 8 Wm^{-2} and -2 Wm^{-2}, for dSST<3.5°C, and much smaller for dSST>3.5°C. In the case of uniform warming (W-R), the change of c_{LW} and G_{clear} per 1°C SST is about the same. Note that the change in G_{clear} is quite different among experiments, indicating the contribution of water vapor distribution over the cold pool.

REFERENCES

Gadgil, S., P. V. Joseph, and N. V, Joshi, 1984: Ocean-atmospheric coupling over monsoon regions. *Nature*, **312**, 141-143.

Graham, N., and T. P. Barnett, 1987: Sea surface temperature, surface wind divergence, and convection over tropical oceans. *Science*, **238**, 657-659.

Kalnay, E., and Coauthors, 1996: The NMC/NCAR 40 year reanalysis project. *Bull. Am. Meteorol. Soc.*, 77, 437-471.

Lau, L.-M., H-T. Wu, S. bony, 1997: The role of large-scale atmospheric circulation in the relationship between tropical convection and sea surface temperature. *J. Climate*, **10**, 381-392.

Lindzen, R. S., M.-D. Chou, A. Hou, 2000: Does the earth have an adaptive infrared iris? submitted.to *Bull. Am. Meteorol. Soc*

Reynolds, R. W., and T. S. Smith, 1994: Improved global sea surface temperature analysis. *J. Climate*. 7, 929-948.

Rossow, W. B., and R. A. Schiffer, 1991: ISCCP Cloud Data Products. *Bull. Am. Meteorol. Soc.*, **72**, 2-20.

Waliser, D. E., 1996: Formation and limiting mechanisms for very high sea surface temperature: Linking the dynamics and thermodyanmics. *J. Climate*, **9**, 161-188.